Research in Pharmaceutical Sciences, April 2026; 21(2): 191-205
Received:07-09-2025
Peer Reviewed: 06-10-2025
Revised: 27-10-2025
Accepted: 27-10-2025
Published: 24-04-2026

School of Pharmacy & Pharmaceutical Sciences
Isfahan University of Medical Sciences

Original Article

Design, synthesis, and biological evaluation of novel aryl isoxazoles as potential Hsp90 inhibitors

Mina Ardestani[1], Fariba Keshavarzipour[1], Maryam Abbasi[2], Afshin Zarghi[3], Mahmoud Aghaei[4], Mehran Ghiaci[5], and Hojjat Sadeghi-Aliabadi[1,*]

[1]Department of Medicinal Chemistry and Pharmaceutical Sciences Research Centre, School of Pharmacy and Pharmaceutical Sciences, Isfahan University of Medical Sciences, Isfahan, Iran. [2]Department of Medicinal Chemistry, Faculty of Pharmacy, Hormozgan University of Medical Sciences, Bandar Abbas, Iran. [3]Pharmaceutical Science Research Center, Faculty of Pharmacy and Pharmaceutical Sciences, Shahid Beheshti University of Medical Sciences, Tehran, Iran. [4]Department of Clinical Biochemistry, School of Pharmacy and Pharmaceutical Sciences, Isfahan University of Medical Sciences, Isfahan, Iran. [5]Department of Chemistry, Isfahan University of Technology, Isfahan, Iran.

Abstract

Background and purpose: Heat shock protein 90 (Hsp90) is a molecular chaperone critical for the stabilization of numerous oncoproteins, making it a promising target for anticancer drug development. This study aimed to design, synthesize, and evaluate novel 3,5-diarylisoxazole derivatives as potential Hsp90 inhibitors

Experimental approach: A series of 3,5-diarylisoxazole compounds ($5R_{1-6}$) was designed using molecular docking to predict binding affinity. Compounds were synthesized *via* cyclization of 4-chloroacetophenone with hydroxylamine hydrochloride, followed by condensation with various aldehydes. Structures were confirmed by melting point, FT-IR, and 1H-NMR spectroscopy. The MTT assay assessed cytotoxicity, and Hsp90 inhibitory activity was evaluated using an Hsp ELISA kit. The stability of the $5R_3$ compound in the Hsp90 active site was investigated using molecular dynamics simulation.

Findings/Results: All compounds showed favorable binding energies. Compound $5R_3$ showed the highest binding affinity (ΔG = -7.83 kcal/mol) and the highest cytotoxicity against MCF-7 cells (IC_{50} = 0.014 µM) and significantly reduced Hsp90 concentration from 5.54 ng/mL (untreated) to 1.56 ng/mL. Furthermore, molecular dynamics simulation studies confirmed the stability of the Hsp90-$5R_3$ complex during a 100 ns simulation.

Conclusion and implications: Compound $5R_3$ with an electronegative substituent (F) on the aromatic ring showed the highest cytotoxic effect, also decreased the concentration of Hsp90 protein more than others.

Keywords: Hsp90 inhibitor; Isoxazole; Molecular docking; Molecular dynamics simulation; MTT assay.

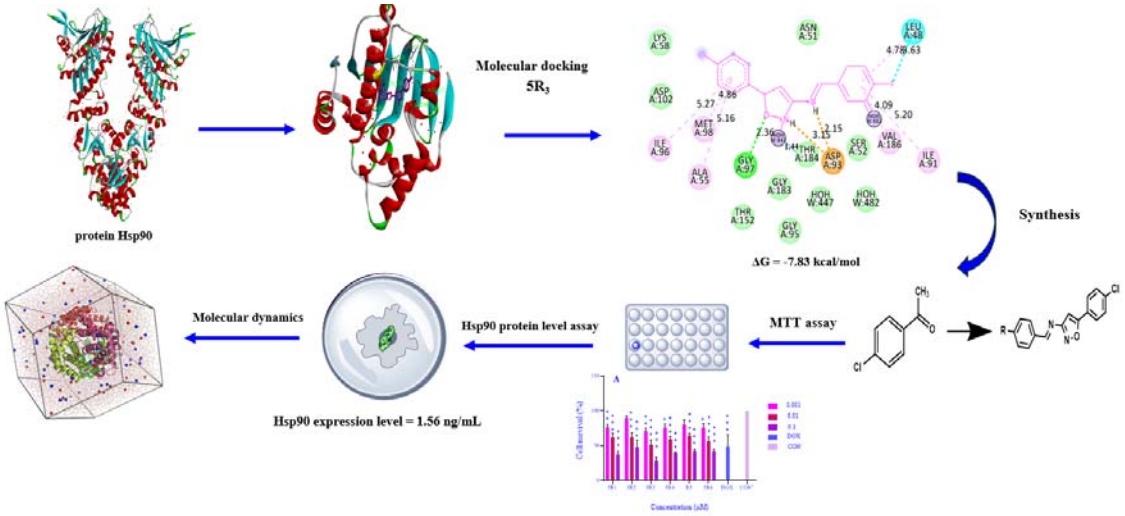

*Corresponding author: H. Sadeghi-Aliabadi
Tel: +98-3137927099, Fax: +98-3136680011
Email: sadeghi@pharm.mui.ac.ir

Access this article online

Website: http://rps.mui.ac.ir

DOI: 10.4103/RPS.RPS_173_25

INTRODUCTION

Heat shock proteins (Hsps) are highly conserved molecular chaperones involved in protein folding, stabilization, and degradation, particularly under stress conditions. Hsps are classified into several families based on their approximate molecular weights, including Hsp100, Hsp90, Hsp70, Hsp60, and small Hsps, each playing distinct roles in protein folding and cellular stress response (1,2). Hsp90, a key member of this family, plays a crucial role in the folding and activation of numerous client proteins implicated in cancer progression. Inhibition of Hsp90 disrupts the stability of these oncoproteins, making it an attractive target for anticancer therapy (3,4). Hsp90 is a homomeric protein composed of two identical subunits with three domains: an N-terminal ATP-binding domain, a central chaperone domain, and a C-terminal dimerization domain. Most Hsp90 inhibitors target the ATP-binding site in the N-terminal domain. Natural inhibitors such as radicicol and geldanamycin, as well as synthetic compounds like luminespib (NVP-AUY922), have demonstrated potent Hsp90 inhibitory activity (5,6).

Radicicol and geldanamycin (Fig. 1) are introduced as the first natural Hsp90 inhibitors. These compounds work by binding directly to the ATP-binding pocket in the N-terminal domain, effectively competing with ATP and disrupting the associated function of Hsp90 (7). Besides these natural compounds, numerous novel compounds have been synthesized that act as Hsp90 inhibitors, especially for anticancer therapy (8). Some recent studies highlight heterocyclic molecules such as pyrazole, indole, pyrimidine, triazole, isoxazole, and thioquinazoline that have shown promising anticancer activity (8-12). Luminespib, containing an isoxazole ring, is a high-affinity Hsp90 inhibitor with an IC_{50} of 21 nM and a Kd of 1.7 nM (Fig. 1). Its impressive potency has led to its evaluation in phase II of clinical trials (7,13). Most of the previously synthesized isoxazole derivatives bear amide or ketone functionalities at positions 3, 4, or 5 of the isoxazole ring, enabling their conjugation with aryl groups. To enhance their cytotoxic potential, certain compounds feature substitutions exclusively at the 3 and 5 positions, where the substituents are either attached directly to the ring or connected via methylene, ethylene, or cyclic linkers. Galiskan *et al.* reported the synthesis of a series of 3,5-diaryl derivatives incorporating a piperazinyl linker, which exhibited cytotoxic activity against the MCF-7 breast cancer cell line within the concentration range of 1.2-20 µM (14). Inspired by the therapeutic potential of isoxazole-based organic molecules (15,16) and our previous works (17,18), we designed and synthesized a novel series of 5-phenylisoxazol-3-amine derivatives to evaluate their cytotoxic and Hsp90 inhibitory activities.

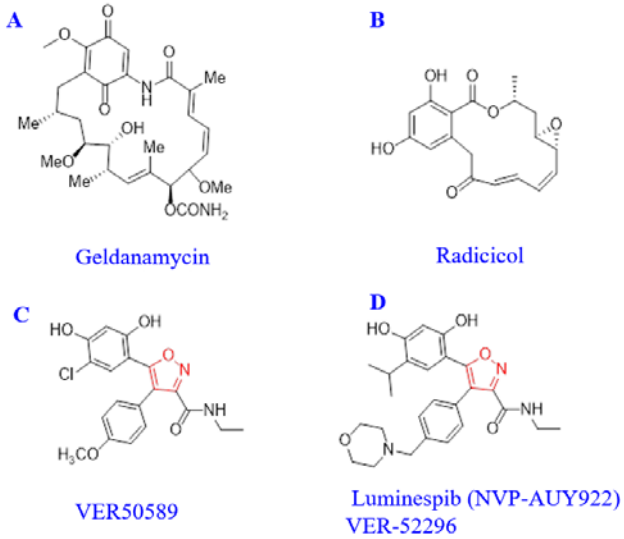

Fig. 1. The chemical structure of some natural (A and B) and synthetic Hsp90 inhibitors with an isoxazole ring (C and D) is being investigated in different stages of clinical trial studies.

MATERIALS AND METHODS

Compounds and instrumentation

All chemicals used in these experiments were sourced from Sigma-Aldrich or Merck and employed without additional purification. Thin-layer chromatography (TLC) was employed to follow the progress of the reaction and confirm the identity and purity of the substances during the experiment. The melting point of the compounds was measured with an electrothermal melting point instrument model 9200. Infrared spectra were obtained by a JASCO Fourier transform infrared spectroscopy (FT-IR, JASCO, Japan) using KBr discs. Compounds were analyzed *via* proton nuclear magnetic resonance (^{1}H-NMR) spectroscopy, conducted with a Bruker Ultra Shield 400 MHz (Bruker, USA) and recorded in $CDCl_3$ solvents.

Molecular docking

In this study, experimental docking of 5-phenylisoxazol-3-amine derivatives as Hsp90 inhibitors was performed using AutoDock 4.2 software (19). The protein structure was obtained from the Protein Data Bank (PDB: 5xqd) (20). Its structure was produced by eliminating all water molecules, except for the water molecules critical for protein-ligand interactions, ions, and ligands. Atomic charges were incorporated and computed *via* the Kollman procedure. The file was saved in pdbqt format. A grid box size of 60 × 60 × 60 Å, centered on the protein binding pocket, with a grid spacing of 0.375 Å, was utilized. The structures of the 3D ligands were illustrated using Marvin Sketch v5.7 software and saved in PDB format. The Gasteiger-Marsili method was employed to compute the partial atomic charges of the ligands. This calculation is crucial as partial charges significantly influence molecular binding by dictating macromolecule-ligand interaction (21). The Lamarckian genetic evolution was executed over 100 iterations. Additionally, parameters about water molecules were integrated into the AD4-parameter and AD4-bound files. All runs were categorized according to the lowest binding energy, and a comprehensive analysis was performed to determine the best conformation and ligand orientation within the protein's active site. The docking procedure was analyzed and visualized utilizing Pymol and Discovery Studio Visualizer version 17.2 (22,23).

Molecular dynamics simulation

Molecular dynamics (MD) simulations were conducted to investigate the stability of the ligand-Hsp90 complex. Following the biological assessments, compound 5R3 was chosen for MD simulations. The simulations aimed to evaluate the stability of $5R_3$ within the Hsp90 active site and to compare its interaction pattern with that of the reference Hsp90 inhibitor AUY-922. MD simulations were performed with GROMACS 2021.5. (24). Protein pKa values were computed with the PROPKA 3.1 web server (25). Protein topology files were prepared using the Amber force field. Ligand topologies were prepared using ACPYPE, which interfaces with antechamber to derive force-field parameters for small molecules (26). Simulations under physiological conditions were performed by solvating the Hsp90-ligand complex in a dodecahedral box containing TIP3P water, followed by the addition of counterions (Na^+ or Cl^-) to achieve charge neutrality. After energy minimization, a two-step equilibration protocol was applied before production MD. The first step was an NVT equilibration at 323 K for 500 ps, and the second step was an NPT equilibration at 323 K and 1 bar for 500 ps. Following system stabilization, a 100 ns MD simulation was conducted at 323 K. Trajectory analyses were examined for time-dependent properties, including backbone root mean square deviation (RMSD), root mean square fluctuations (RMSF), and radius of gyration (Rg).

General synthesis procedure of compounds

Synthesis of (Z)-3-chloro-3-(4-chlorophenyl) acrylonitrile (2)

Phosphoryl chloride ($POCl_3$; 16.6 mmol, 1.6 mL) was added dropwise to 13 mL of dry dimethylformamide (DMF) while keeping the temperature below 25 °C using an ice bath, and it was stirred for 30 min. Then 4-chloroacetophenone (8.3 mmol, 1.2 mL) was added dropwise, while the temperature was maintained at 60 °C. After that, the reaction mixture was stirred at room temperature for 2 h. Then, hydroxylamine hydrochloride (33.32 mmol, 2.1 g) was added dropwise (exothermic reaction), and the reaction was stirred for

another 24 h at room temperature. The progress of the reaction was followed by TLC. After the completion of the reaction, the mixture was poured into crushed ice to obtain a solid product. The resulting product was filtered, washed with cold ethanol, dried, and recrystallized from ethanol to obtain an off-white solid product (76% yield) (27,28).

Synthesis of (4-chlorophenyl) isoxazol-3-amine (3)

(Z)-3-chloro-3-(4-chlorophenyl) acrylonitrile (2) (10 mmol, 1.2 g) was dissolved in ethanol (10 mL) and stirred for a few min. Sodium hydroxide (96%) and hydroxylamine hydrochloride (15 mmol, 1.5 g) were then added, and stirred to mix while the pH was kept between 7 and 8. The reaction was then heated to 60 °C and stirred for another 24 h. HCl (3 mmol) was added in one portion, and the reaction was heated for 2 h at 80 °C. Then, the reaction was allowed to cool down to room temperature. The aqueous layer was extracted with EtOAc (2 × 200 mL). The organic layer was dried using $MgSO_4$ and evaporated to crystallize. Finally, the product was recrystallized from ethanol to give a white powder with a 78% yield (29,30).

Synthesis of (4-chlorophenyl) isoxazol-3-amine derivatives coupled with various aldehydes ($5R_{1-6}$)

The final Schiff base products were prepared by mixing equimolar amounts (1 mmol) of the aldehyde derivatives (4) and (4-chlorophenyl) isoxazol-3-amine (3) in absolute ethanol (10 mL) under reflux. After the reaction was completed (checked by TLC), the solvent volume was reduced by evaporation, cooled down to room temperature, and filtered. The obtained solid product was washed several times with cold methanol and recrystallized from a mixture of ethanol and water to give compounds $5R_{1-6}$ as illustrated in Table 1.

Table 1. The structure, chemical formula, yield, and melting point of synthesized compounds $5R_{1-6}$

Compound code	Structure	Chemical formula	Purified compounds yield (%)	Melting point (°C)
$5R_1$	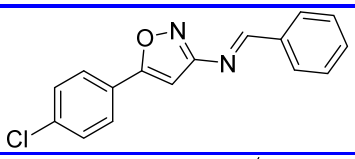	$C_{16}H_{11}ClN_2O$	25	195
$5R_2$	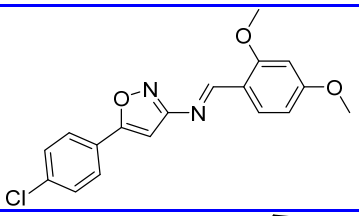	$C_{18}H_{15}ClN_2O_3$	25	247
$5R_3$	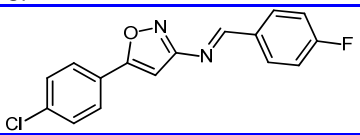	$C_{16}H_{10}ClFN_2O$	55	233
$5R_4$	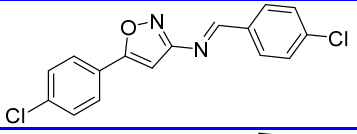	$C_{16}H_{10}Cl_2N_2O$	45	231
$5R_5$	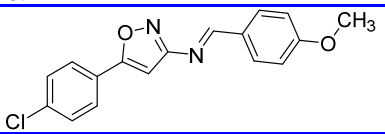	$C_{17}H_{13}ClN_2O_2$	37	235
$5R_6$	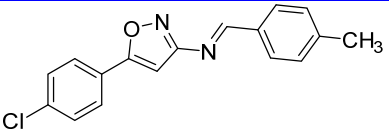	$C_{17}H_{13}ClN_2O$	40	224

Biological evaluations

Cell lines

Cancerous cells, including HeLa (cervical cancer) and MCF-7 (breast cancer), and a normal cell line, HUVEC, were purchased from the Pasteur Institute (Tehran, Iran). HeLa cells were maintained in Dulbecco's Modified Eagle Medium (DMEM), while HUVEC and MCF-7 cells were maintained in RPMI 1640 medium, at 37 °C in a humidified atmosphere (containing 5% CO_2). Media were completed with 10% fetal bovine serum (FBS), 100 units/mL penicillin, and 100 µg/mL streptomycin.

Cytotoxic activity assay

MTT assay was performed to evaluate cell viability and cytotoxic effects of the tested compounds against cancer cells as reported before (31). Briefly, cells were seeded (5×10^3 cells/well) in 96-well plates and incubated for 24 h. After that, the cells were treated with different concentrations of synthesized compounds (0.001, 0.01, and 0.1 µM) and incubated for 48 h. After the exposure period, 20 µL of MTT reagent (5 mg/mL) was added to each well, and incubation continued for an additional 3 h. Subsequently, 150 µL of dimethyl sulfoxide (DMSO) was replaced with media to dissolve the formed formazan crystals, and absorbance was measured at 570 nm using an enzyme-linked immunosorbent assay (ELISA) plate reader (BioTek, USA). Experiments were conducted in triplicate, and cell viability was calculated by comparing treated samples against negative controls. Doxorubicin (2 µg/mL) served as the positive control to validate assay performance.

Hsp90 protein level assay

The effect of synthesized cytotoxic agents on Hsp90 expression levels was evaluated using the Hsp90 expression level kit (Cusabio, USA), in accordance with the manufacturer's protocol. Standards and samples were added to the designated wells with a concentration of one-fourth of IC_{50} values and incubated at 37 °C for 2 h. After incubation, the supernatant was discarded and replaced with 100 µL of biotin-conjugated antibody, followed by a 1-h incubation at 37 °C. The wells were then aspirated and washed three times with 400 µL of the provided wash buffer.

Subsequently, 100 µL of horseradish peroxidase-conjugated avidin (HRP-avidin) was added to each well and incubated for another hour at 37 °C. The washing procedure was repeated as described above. Then, 90 µL of 3,3',5,5'-tetramethylbenzidine (TMB) substrate solution was introduced into the wells and allowed to react for 15-30 min at 37 °C. The reaction was terminated by adding the stop solution, and absorbance was measured at 450 nm using an ELISA plate reader (BioTek, USA).

Statistical analysis

IC_{50} values were calculated by linear regression and expressed as mean ± SD. All linear regressions in this paper were analyzed using GraphPad Prism 6 software (32). Statistical analysis was performed using one-way analysis of variance (ANOVA) followed by Tukey's post hoc test to determine the significant differences among the groups. $^*P \leq 0.05$ values were considered statistically significant.

RESULTS

Docking studies

Molecular docking analysis was performed to investigate the binding interactions between the drugs and the Hsp90 binding site. The results, including binding free energies (ΔG), electrostatic interactions, hydrogen binding, and hydrophobic interactions, are summarized in Table 2. To validate the docking protocol, the NVP-AUY922 compound, as a reference and crystallographic ligand were re-docked. Co-crystal ligand occupies the Hsp90 active site in a manner that is surrounded by essential amino acids such as Asp93, Gly97, Thr184, Ala55, Val186, Met98, Ile91, and Ile96, along with structural water molecules. A crystallographic ligand with binding energies (ΔG: -7.09) and a hydrogen bond is formed with the oxygen of the isoxazole ring with amino acid Gly97 at a distance of 2.86 Å and amino acid Asp93 at a distance of 1.69 Å. In compound NVP-AUY922, hydrogen bonds are formed by the oxygen group of the isoxazole ring with amino acid Thr184 at a distance of 2.04 Å and amino acid Asp93 at a distance of 1.80 Å, and by water molecule 447 at a distance of 2.70 Å and water molecule 482 at a distance of 2.55 Å.

Table 2. Binding energy (ΔG), hydrophobic and hydrophilic interactions of synthesized compounds and NVP-AUY922 in the active site of Hsp90 protein.

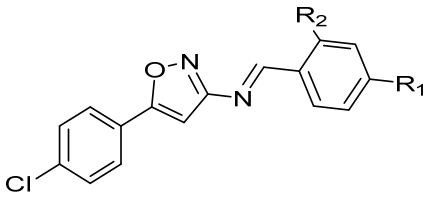

Compounds	R_1	R2	(ΔG) (kcal/mol)	H-Bond amino acids (distance A^0)	Electrostatic amino acids	Hydrophobic Amino Acids
Luminespib (NVP-AUY922)	-	-	-12.42	Gly97 (2.27), Thr184 (2.09), Asp93 (1.80)	Met98	Ala55, Lys58, Ile96, Val186
Co-crystal ligand	-	-	-7.09	Gly97 (2.86), Asp93 (1.69)	Met98	Ala55, Lys58, Ile96
$5R_1$	H	H	-6.78	Leu107 (2.14), Thr184 (1.59)	Asp102, Met98	Leu48, Val186, Ile96
$5R_2$	OCH_3	OCH_3	6.47-	Gly97 (2.26), Lys58 (2.51)	Asp102, Met98	Ala55
$5R_3$	F	H	-7.83	Gly97 (2.36), Thr184 (1.44)	Asp93	Ala55, Val186, Met98, Ile91-96
$5R_4$	Cl	H	-6.78	Leu107 (2.09)	Asp93, Met98	Ile96, Val186, Leu48
$5R_5$	OCH_3	H	-6.43	Leu107 (2.12)	Met98	Ala55
$5R_6$	CH_3	H	-6.65	Leu107 (2.15)	Met98	Val186, Ile96

Hydrophobic interactions of the ligand with Ala55, Lys58, Ile96, Val186, and the formation of electrostatic interactions with Met98 are shown in Fig. 2. The RMSD between the experimental and predicted states was calculated. The RMSD value obtained was 1.4 Å, indicating good accuracy and reliability of the docking method.

Synthesis of compounds

The target compounds were synthesized through a three-step synthetic route as illustrated in the synthetic scheme (Fig. 3).

In step 1, the initial ketone (compound 1) was subjected to the Vilsmeier-Hack reaction using DMF and $POCl_3$ in the presence of hydroxylamine hydrochloride to produce intermediate compound 2, containing a chlorinated aromatic moiety and a cyano substituent (33). Step 2 involved the conversion of compound 2 to the isoxazole derivative 3 *via* reaction with sodium hydroxide and ethanol in the presence of hydroxylamine hydrochloride, which resulted in ring closure and formation of the amino-isoxazole scaffold. Finally, in step 3, compound 3 was subjected to condensation with various substituted benzaldehydes (compound 4) in ethanol under acidic conditions to provide the final Schiff base derivatives $5R_{1-6}$, as shown in the Fig. 3. This multi-step synthesis efficiently provided the desired compounds with the designed substitution pattern. The lower yields obtained for some final derivatives can be explained by side-product formation and purification difficulties.

(E)-N-(5-(4-chlorophenyl)isoxazol-3-yl)-1-phenylmethanimine ($5R_1$)

$C_{16}H_{11}ClN_2O$; molecular weight (MW): 282.73 Da; melting point (m.p.):195 °C; yield: 25%; IR (KBr): ɣ (cm^{-1}) 1622 (N=CH); ^{1}H-NMR (400 MHz, $CDCl_3$) δ 9.59 (s, 1H, N=CH), 7.63 (m, 4H, Ar), 7.47 (m, 5H, Ar), 6.04 (s, 1H, CH).

(E)-N-(5-(4-chlorophenyl)isoxazol-3-yl)-1-(2,4-dimethoxyphenyl)methanimine ($5R_2$)

$C_{18}H_{15}ClN_2O_3$; MW: 342.78 Da; m.p.: 247 °C; yield: 25%; IR (KBr): ɣ (cm^{-1}) 1622 (N=CH); ^{1}H-NMR (400 MHz, $CDCl_3$) δ 7.75 (d, *J* = 2.2 Hz, 1H, N=CH), 7.68 (m, 2H, Ar), 7.46 (m, 3H, Ar), 7.40 (m, 2H, Ar) 6.96 (d, *J* = 8.4 Hz, 1H,CH), 3.99(d, *J* = 10.7 Hz, 6H, OCH_3).

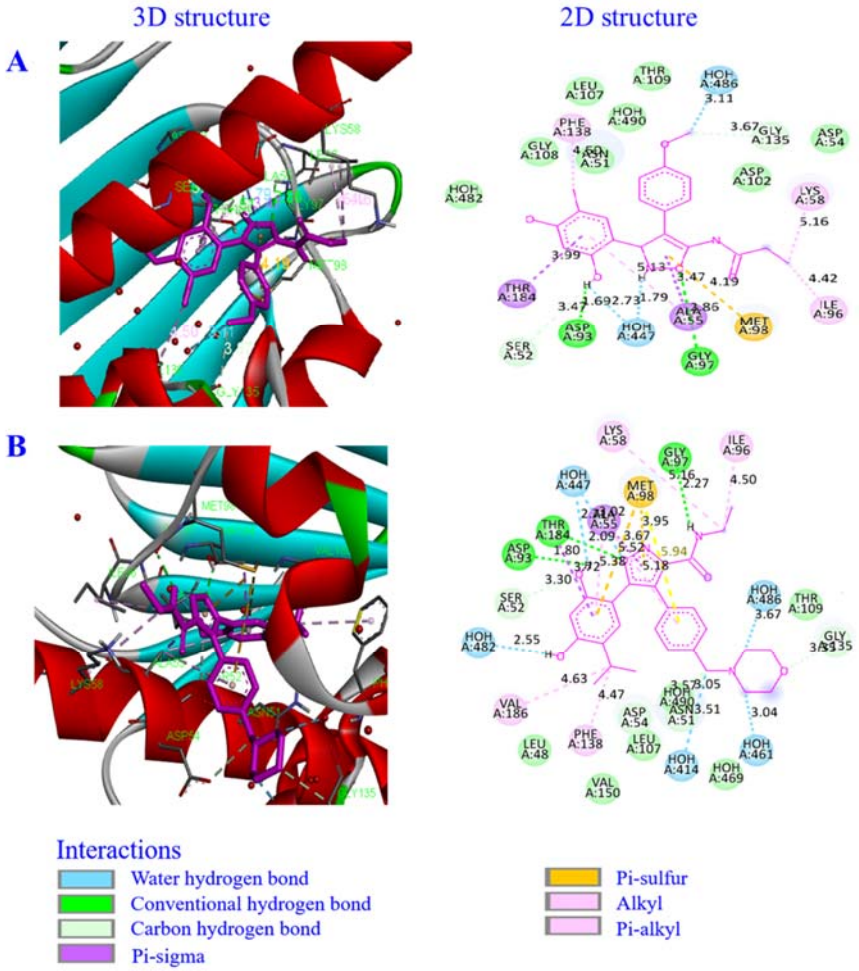

Fig. 2. The illustration of the binding mode of 3D and 2D structures of compounds A (co-crystal ligand) and B (NVP-AUY922) in the active site of Hsp90 protein.

Fig. 3. Scheme of different steps in the synthesis of desired compounds.

(E)-1-(4-chlorophenyl)-N-(5-(4-chlorophenyl) isoxazol-3-yl)methanimine (5R3)

$C_{16}H_{10}Cl_2N_2O$; MW: 317.17 Da; m.p.: 231 °C; yield: 55%; IR (KBr): ɣ (cm^{-1}) 1622 (N=CH); ^{1}H-NMR (400 MHz, $CDCl_3$) δ 8.83 (s, 1H, N=CH), 7.93 (m, 2H, Ar), 7.78 (dd, *J* = 9.0, 2.6 Hz, 2H, Ar), 7.51 (d, *J* = 7.5 Hz, 4H, Ar), 6.64 (d, *J* = 2.9 Hz, 1H, CH).

(E)-N-(5-(4-chlorophenyl)isoxazol-3-yl)-1-(4-fluorophenyl)methanimine (5R4)

$C_{16}H_{10}ClFN_2O$; MW: 300.72 Da; m.p.: 233 °C; yield: 45%; IR (KBr): ɣ (cm^{-1}) 1607 (N=C); ^{1}H-NMR (400 MHz $CDCl_3$) δ 8.83 (s, 1H, N=CH), 7.94 (dd, *J* = 8.6, 2.3 Hz, 2H, Ar), 7.78 (dd, *J* = 9.0, 2.6 Hz, 2H, Ar), 7.51 (m, 4H, Ar), 6.64 (d, *J* = 2.8 Hz, 1H, CH).

(E)-N-(5-(4-chlorophenyl)isoxazol-3-yl)-1-(4-methoxyphenyl)methanimine (5R5)

$C_{17}H_{13}ClN_2O2$; MW: 312.75 Da; m.p.: 235 °C; yield: 37%; IR (KBr): ɣ (cm^{-1}) 1607 (N=C); ^{1}H-NMR (400 MHz, $CDCl_3$) δ 9.81 (s, 1H, N=CH), 7.84 (dd, *J* = 8.8, 3.5 Hz, 2H, Ar), 7.70 (m, 2H, Ar), 7.12 (m, 2H, Ar), 7.04 (m, 2H, Ar), 6.18 (s, 1H, CH), 3.81(s,1H,OCH_3).

(E)-N-(5-(4-chlorophenyl)isoxazol-3-yl)-1-(p-tolyl)methanimine (5R6)

$C_{17}H_{13}ClN_2O$; MW: 296.75 Da; m.p.: 224 °C; yield: 40%; IR (KBr): ɣ (cm^{-1}) 1607 (N=C); ^{1}H-NMR (400 MHz, $CDCl_3$) δ 8.24 (m, 1H, N=CH), 8.09 (m, 2H, Ar), 7.69 (m, 2H, Ar), 7.56 (t, *J* = 7.9 Hz, 2H, Ar), 7.36 (m, 2H, Ar), 6.64 (s, 1H, CH), 2.78(s, 3H, CH_3).

Biological assays

The biological activities of the synthesized compounds were assessed through *in vitro* assays, including cytotoxicity evaluation and ELISA-based quantification of Hsp90 expression levels. The antiproliferative effects of the six synthesized compounds were evaluated using the MTT assay against MCF-7, HeLa, and HUVEC cell lines (Fig. 4).

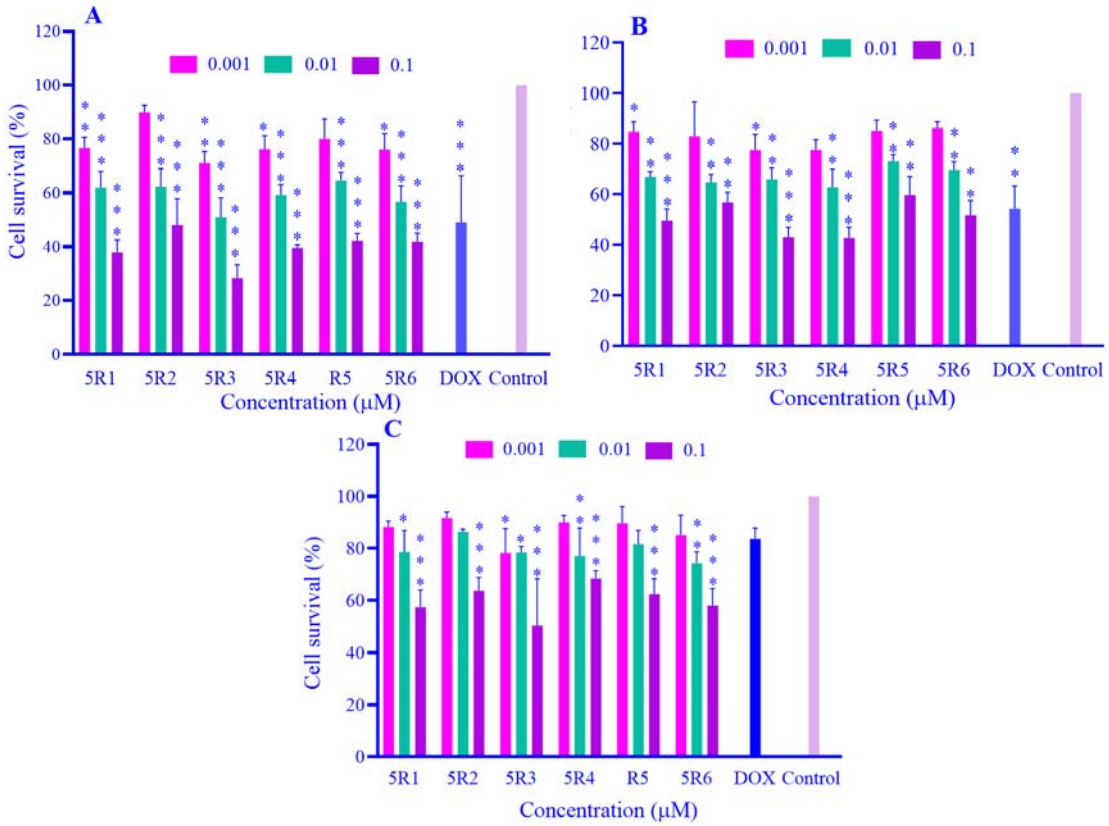

Fig. 4. Cytotoxicity assessment of synthesized isoxazole derivatives against (A) MCF-7, (B) HeLa, and (C) HUVEC cell lines using the MTT assay. Data are expressed as mean ± SD, n = 3. *$P \leq 0.05$, **$P \leq 0.01$, ***$P \leq 0.001$ indicate significant differences compared to the control group. DOX, Doxorubicin.

As shown in Fig. 4, among the six compounds, 5R3 showed the highest antiproliferative activity with IC50 of 0.014 ± 0.002 µM, 0.050 ± 0.010 µM, and 0.150 ± 0.030 µM against MCF-7, HeLa, and HUVEC, respectively. We used an ELISA kit to detect the intracellular Hsp90 protein level. For this purpose, the compounds with the highest cytotoxicity (5R$_3$ and 5R$_4$ at a concentration of ×0.25 IC50) were used and the results are shown in Fig. 5. As seen in this figure, the level of expression of Hsp90 proteins was reduced from 5.5 ± 1.10 ng/mL in untreated cells (negative control) to 1.5 ± 0.15 and 4.8 ± 0.70 ng/mL by compounds 5R3 and 5R1, respectively.

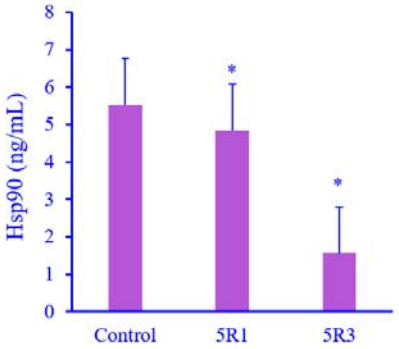

Fig. 5. Inhibitory effects of compound5R$_1$ and 5R$_3$ on Hsp90 protein levels in MCF-7. Un-treated cells were used as a negative control. Data represent the mean ± SD of three independent experiments (n = 3). *$P \leq 0.05$ indicates significant differences compared to the control group.

MD simulation

A 100 ns MD simulation was conducted. To evaluate backbone stability of the Hsp90-ligand complexes, the RMSD was computed for the ligand 5R$_3$, the Hsp90 protein, and the reference inhibitor AUY-922. As shown in Fig. 6A, the RMSD trajectories for the 5R$_3$-Hsp90 complex, the Hsp90 protein, and the Hsp90 inhibitor were nearly superimposable in the initial 50 ns, indicating similar early-stage conformational stability. RMSD analysis shows that AUY922 bound to Hsp90 exhibits greater stability than both apo Hsp90 and Hsp90 in complex with 5R$_3$ for the remainder of the simulation. Notably, 5R$_3$ displays fluctuations under 0.3 nm, reflecting its stability in the Hsp90 active site. Figure 6B presents the RMSF of the Hsp90 protein, where lower values correspond to greater residue stability. The active-site residues Asn51, Met98, Ala55, Asp93, Leu107, Phe138, Asn106, and Thr184 exhibited stable behavior across the three independent simulations, indicating stability of the backbone in the Hsp90 active site. Figure 6C presents the Rg for the two Hsp90-ligand complexes and the apo protein. The Rg trajectories were highly similar across systems, with conserved coherence over the entire simulation, suggesting compactness of the Hsp90 backbone during MD simulation.

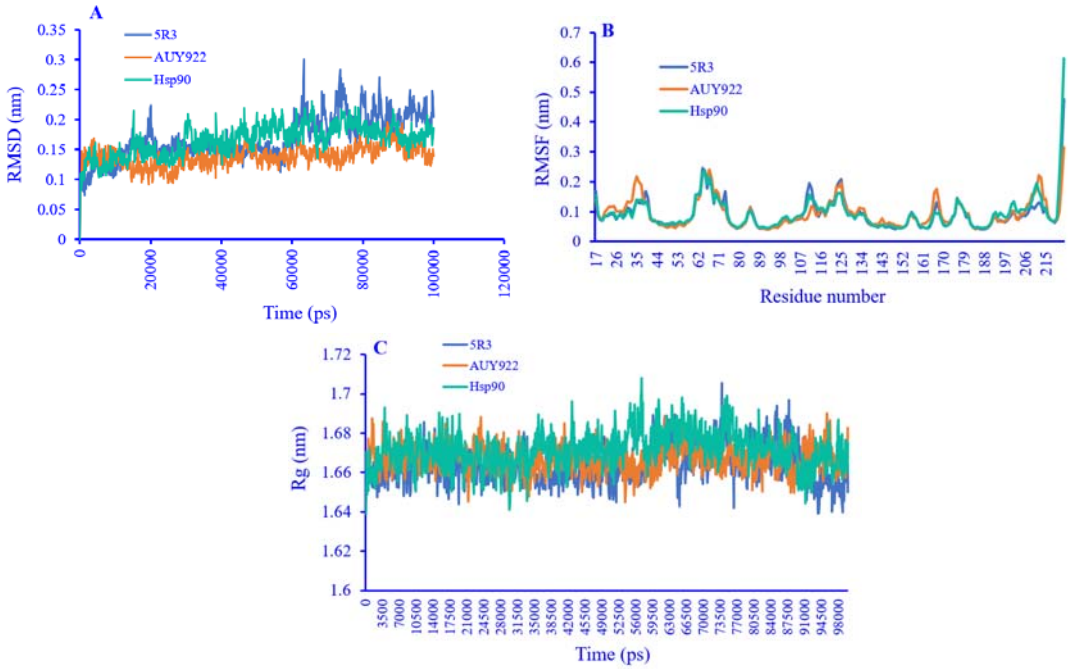

Fig. 6. (A) RMSD plot; (B) RMSF plot; and (C) Rg plot of the Hsp90 protein backbone in complex with compounds 5R$_3$, AUY-922, and Hsp90 protein. RMSD, Root mean square deviation; RMSF, root mean square fluctuations; Rg, radius of gyration.

DISCUSSION

Most previously synthesized isoxazole derivatives feature the isoxazole ring linked to aryl groups directly or *via* amide bonds to an aliphatic group; however, ethylenic and imine linkages have also been reported, occasionally enhancing biological activity. For example, converting the two carbonyl groups in curcumin into an isoxazole ring significantly improved its cytotoxicity against MCF-7 cells, reducing IC_{50} from 21.89 to 3.97 µM (34). Balaji *et al*. conjugated Hispolon with an isoxazole ring, resulting in enhanced anti-tuberculosis activity (MIC = 1.6 µg/mL) (35). Yin and colleagues linked isoxazole to chalcone and observed moderate activity against melanoma cells (IC_{50} = 135 µM) (36). Arylation of isoxazole *via* imine bonds at positions 3 and 4 produced compounds more potent than erlotinib against A549 cells, with IC_{50} improving from 25 to 17 µM (37). Additionally, conjugation with N-aryl pyrazole yielded a derivative exhibiting strong cytotoxicity (IC_{50} = 0.31 µM) toward MCF-7 cells (38). Furthermore, our compounds are 5-aryl substituted isoxazoles that contain fluorine and chlorine, electron-rich substituents, that create stronger electrostatic and hydrophobic interactions with additional residues such as Asn51, Asp58, Met98, and Val150 in the Hsp90 pocket. Mechanistically, unlike previous inhibitors, our fluorinated analogs significantly reduce Hsp90 expression in cancer cells (down to 1.56 ng/mL) while maintaining lower cytotoxicity in normal cells, indicating a distinct modulation profile of the chaperone cycle rather than a complete ATP-competitive inhibition (38).

Imines, especially those attached to aromatic rings, have shown significant potential as anticancer agents through various mechanisms such as induction of apoptosis, production of reactive oxygen species (ROS), and disruption of vital cellular functions (39,40). They have also shown the ability to suppress the growth of MCF-7 cells and are considered promising anticancer candidates (41). The imine group, with its C=N double bond, is highly polar, allowing interaction with key amino acid residues such as Asp93, Thr184, and Lys5 (42). Imines can also act as intermediate rings between aryl or heterocyclic groups and are relatively stable in aqueous and cellular environments, making them suitable for the design of selective and cell-penetrating inhibitors (40). Building upon previous findings and our molecular docking studies of the designed compounds, and considering the novelty of the approach, this study focused on synthesizing isoxazole derivatives functionalized with aryl groups *via* imine bonds at positions 3 and 5, followed by evaluation of their cytotoxicity and effects on Hsp90 protein expression.

The interaction of the novel isoxazole derivatives with the Hsp90 protein binding site was investigated by docking studies, the dominant method for predicting their function. As shown in Table 2, all synthesized compounds occupy the Hsp90 active site in a manner that is surrounded by essential amino acids such as Asp93, Gly97, Thr184, Ala55, Val186, Met98, Ile91, and Ile96, along with structural water molecules. Among the designed derivatives in compound $5R_1$, hydrogen bonds are formed directly by the NH group of the isoxazole ring with amino acid Leu107 at a distance of 2.14 Å and indirectly by crystallographic water with Thr184 at a distance of 1.59 Å. Hydrophobic interactions of the ligand with Leu48, Val186, and Ile96 and the formation of electrostatic interactions of the isoxazole ring oxygen with Met98 are shown. Compound $5R_4$ forms hydrogen bonds *via* the NH group of the isoxazole ring with the amino acid residue Leu107 at a distance of 2.09 Å and with a crystallographic water molecule at a distance of 2.64 Å. This ligand makes hydrophobic interactions with Val186, Leu48, and Ile96 and electrostatic interactions with the amino acid Met98. Compound $5R_3$ forms hydrogen bonds directly through the oxygen of the isoxazole ring to amino acid Gly97 at a distance of 2.36 Å and indirectly *via* a crystallographic water to Thr184 at a distance of 1.44 Å. This ligand makes hydrophobic interactions with Ala55, Val186, Met98, Ile91, and Ile96, and the N group makes electrostatic interactions with the amino acid Asp93, which are shown in Table 3. Both the optimized $5R_3$ structure (ΔG = -7.83) and the co-crystal structure (ΔG = -7.09) showed acceptable binding energies.

Table 3. The illustration of the binding mode of compounds $5R_1$, $5R_3$ and $5R_4$ (3D and 2D structures) in the active site of Hsp90 protein, derived from AutoDock4.

Compound No.	3D structure	2D structure
$5R_1$	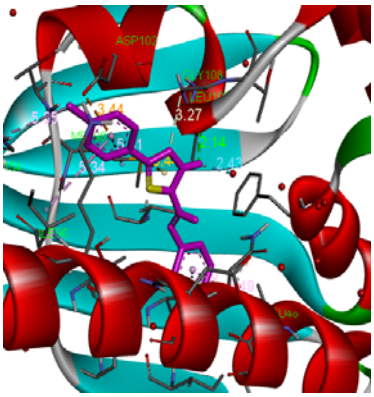	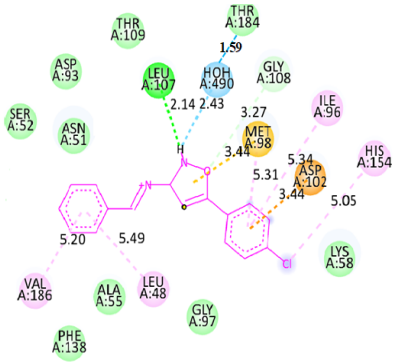
$5R_4$	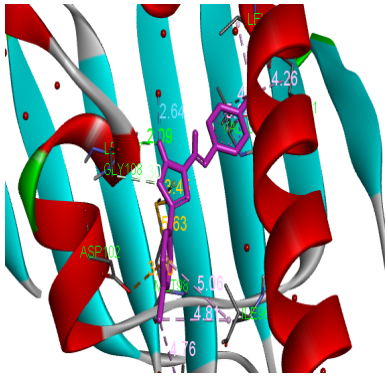	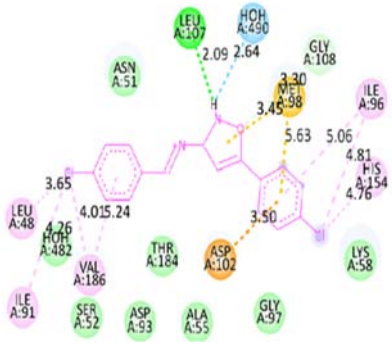
$5R_3$	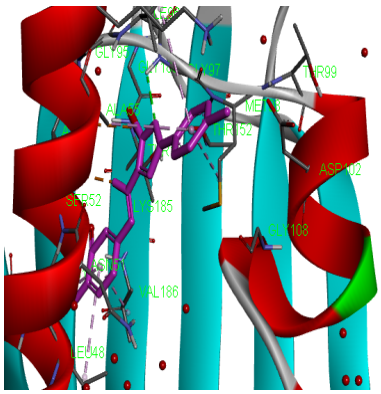	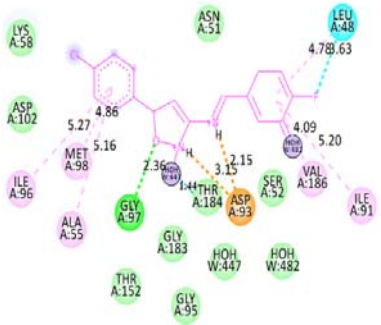
Interactions	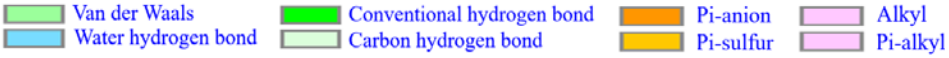	

The key interactions underlying this stability included hydrogen bonding between the oxygen atom of the isoxazole ring and the amino acid Gly97 in both complexes. In addition, hydrophobic interactions were present with the essential amino acids of the active site, particularly Ala55, Val186, and Ile91-96. The binding ΔG of the proposed derivatives was as follows: NVP-AUY922 > $5R_3$ > co-crystal ligand > $5R_1$ and $5R_4$ > $5R_6$ > $5R_2$ > $5R_5$.

In this study, six isoxazole derivatives (compounds $5R_{1-6}$) were synthesized following the procedure outlined in Fig. 3. These imine-functionalized isoxazole derivatives were created by condensing 4-chlorophenylisoxazol-3-amine with various aldehydes.

The presence of the imine group (N=CH) was confirmed through IR spectra, which revealed characteristic absorption bands in the range of 1607-1622 cm^{-1}, indicating the C=N stretching vibration.

^{1}H-NMR spectra for both intermediate and final products were recorded in $CDCl_3$, with proton signal assignments detailed in the experimental section. The aromatic and aliphatic protons of the various derivatives appeared within their expected chemical shift ranges. Notably, the imine proton peaks (N=CH) for the different derivatives resonated between 7.25 and 9.81 ppm, and the aromatic proton peaks of the derivatives were observed between 7.04 and 8.09 ppm.

In this study, the cytotoxic effects of the synthesized isoxazole derivatives were evaluated using the MTT assay against two cancer cell lines (MCF-7 and HeLa), along with the normal human umbilical vein endothelial cells, HUVEC. The IC_{50} values were calculated to quantify the potency of each compound (43). Generally, most tested compounds demonstrated significant cytotoxic activity against cancer cell lines at concentrations ≥ 0.01 µM.

As depicted in Fig. 4A, compounds $5R_3$, $5R_1$, and $5R_4$ exhibited pronounced cytotoxicity against MCF-7 cells with IC_{50} values of 0.014 ± 0.002, 0.029 ± 0.080, and 0.030 ± 0.005 µM, respectively. Moderate activity was observed for $5R_6$, $5R_5$, and $5R_2$, with IC_{50} values of 0.031, 0.045, and 0.063 µM, respectively. Against HeLa cells (Fig. 4), all derivatives (except for $5R_2$ and $5R_5$) at concentrations> 0.1 µM showed cytotoxic effects; however, compounds $5R_3$ and $5R_1$ showed IC_{50} values of 0.050 ± 0.01 and 0.080 ± 0.06 µM, respectively. Similarly, compounds $5R_2$, $5R_5$, and $5R_6$ displayed the lowest cytotoxicity against HeLa cells, with IC_{50} values exceeding 0.1 µM. Here, our findings are consistent with previous studies investigating the cytotoxic effects of pyrazole- and isoxazole-based Hsp90 inhibitors such as VER-49009 and VER-50589 (44). In a study by Sharp *et al*. (45), the pyrazole derivative VER-49009 inhibited the growth of the MCF-7 cell line at an effective concentration (GI_{50} = 1360 nM), whereas the isoxazole analogue VER-50589 suppressed the same cell line at a much lower concentration (GI_{50} = 197 nM), which is closer to the potency of compound $5R_3$ observed in our study (IC_{50} = 14 nM). In this regard, Sun *et al.* reported that Luminespib, an isoxazole-containing compound, exhibited cytotoxic activity against MCF-7 and HeLa cells by 50% at concentrations of 6.4 nM and 7.7 nM, respectively (46). In agreement with their findings, our results indicated that the synthesized compounds exhibited significantly higher cytotoxicity toward MCF-7 cells compared to HeLa cells (Fig. 4A and B).

The compounds synthesized in our study contained an isoxazole ring linked to an imine moiety, none of which exhibited cytotoxic effects against the normal HUVEC cell line up to a concentration of 0.1 µM. (Fig. 4C). In contrast, Sharp and colleagues evaluated the compound VER-50589, possessing an isoxazole ring without an imine group, against the same cell line and reported significant cytotoxicity (GI_{50} = 19 nM) (45). These findings suggest that isoxazole derivatives conjugated with an imine group may exhibit enhanced selectivity towards cancer cell lines over normal cells.

The cytotoxicity of all compounds tested in this study against the examined cancer cell lines was concentration-dependent, although compounds $5R_3$ and $5R_1$ demonstrated notably higher efficacy. Based on these findings, these two compounds were identified as promising isoxazole derivatives warranting further investigation.

The intracellular levels of Hsp90 protein were quantitatively measured using a commercially available ELISA kit to evaluate the effect of the synthesized compounds on Hsp90 expression (18). Cytotoxic compounds $5R_1$ and $5R_3$ were selected for treatment, and their impact on Hsp90 protein concentration in cancer cell lysates was assessed relative to untreated controls. The ELISA results demonstrated a significant reduction in Hsp90 levels in cells treated with $5R_1$ and $5R_3$, exhibiting concentrations of 4.85 ± 0.70 and 1.56 ± 0.15 ng/mL, respectively, compared to 5.54 ± 1.10 ng/mL in control cells (Fig. 5). Notably, compound $5R_3$ emerged as the most potent Hsp90 inhibitor among the synthesized derivatives (Fig. 5), displaying significant activity at a concentration of 0.25 × of IC_{50} in MCF-7 cells which was in line with the results

of previous studies (47,48). MD simulations across 100 ns showed that $5R_3$ remains firmly positioned in the ATPase active-site pocket, indicating robust binding stability. Supported by its cytotoxic activity and Hsp90 inhibition, the imine-isoxazole derivative 5R3 emerges as a promising lead compound for the development of novel anticancer therapeutics targeting Hsp90.

CONCLUSION

In this study, a novel series of 5-aryl isoxazole derivatives containing an imine moiety was rationally designed and synthesized as potential Hsp90 inhibitors. Molecular docking studies demonstrated that these derivatives effectively bind to the Hsp90 active site through a combination of hydrogen bonds, electrostatic, and hydrophobic interactions, underscoring their potential as targeted anticancer agents. Structural elucidation was confirmed *via* IR and ^{1}H-NMR spectroscopy. The cytotoxicity evaluation revealed that the most potent compound $5R_3$, containing an F pharmacophore moiety, exhibited a strong affinity for Hsp90, lowering its concentration to approximately 1.5 ng/mL and inhibiting MCF-7 cell proliferation with an IC_{50} of 0.014 ± 0.002 µM. Additional MD analyses confirmed that these compounds maintained stable occupancy within the Hsp90 ATPase active site throughout the simulation. These promising *in-vitro* outcomes position these isoxazole-imine derivatives as viable leads for optimization in the development of selective Hsp90 inhibitors. Nevertheless, to progress toward clinical relevance, further optimization, comprehensive *in vivo* assessment, and mechanistic investigations are warranted to enhance efficacy, selectivity, and pharmacokinetic profiles.

Acknowledgments

This research was financially supported by the Vice Chancellor for Research of Isfahan University of Medical Sciences, Isfahan, Iran, under Grant No. 3991083.

Conflicts of interest statement

All authors declared no conflict of interest in this study.

Authors' contribution

H. Sadeghi Aliabadi designed and supervised the project. M. Ardestani performed the experiments, analyzed, and interpreted the data. F. Keshavarzipour assisted with spectral interpretation and manuscript writing. M. Abbasi contributed to the molecular docking study. A. Zarghi helped synthesize the compounds. M. Aghaei advised on the biological studies, and M. Ghiaci was the advisor for compound synthesis. All authors have read and approved the finalized article. Each author has fulfilled the authorship criteria and affirmed that this article represents honest and original work.

AI declaration

In this article, artificial intelligence tools were used to rewrite and refine certain sentences.

REFERENCES

1. Jee H. Size dependent classification of heat shock proteins: a mini-review. J Exerc Rehabil. 2016;12(4):255-259. DOI: 10.12965/jer.1632642.321.
2. Kregel KC. Heat shock proteins: modifying factors in physiological stress responses and acquired thermotolerance. J Appl Physiol. 2002; 92(5):2177-2186. DOI: 10.1152/japplphysiol.01267.2001.
3. Schopf FH, Biebl MM, Buchner J. The HSP90 chaperone machinery. Nat Rev Mol Cell Biol. 2017;18(6):345-360. DOI: 10.1038/nrm.2017.20.
4. Zuehlke AD, Moses MA, Neckers L. Heat shock protein 90: its inhibition and function. Philos Trans R Soc B Biol Sci. 2018; 373(1738):20160527,1-6. DOI: 10.1098/rstb.2016.0527.
5. Wang M, Shen A, Zhang C, Song Z, Ai J, Liu H, *et al*. Development of heat shock protein (Hsp90) inhibitors to combat resistance to tyrosine kinase inhibitors through HSP90-kinase interactions. J Med Chem. 2016;59(12):5563-5586. DOI: 10.1021/acs.jmedchem.5b01106.
6. Bhat R, Tummalapalli SR, Rotella DP. Progress in the discovery and development of heat shock protein 90 (Hsp90) inhibitors: Miniperspective. J Med Chem. 2014;57(21):8718-8728. DOI: 10.1021/jm500823a.
7. Ardestani M, Khorsandi Z, Keshavarzipour F, Iravani S, Sadeghi-Aliabadi H, Varma RS. Heterocyclic compounds as Hsp90 inhibitors: a perspective on anticancer applications. Pharmaceutics. 2022;14(10):2220. DOI: 10.3390/pharmaceutics14102220.
8. Kitson RRA, Moody CJ. Learning from nature:

advances in geldanamycin-and radicicol-based inhibitors of Hsp90. J Org Chem. 2013;78(11):5117-5141. DOI :10.1021/jo4002849.
9. Cherfaoui B, Guo T, Sun H-P, Cheng W-L, Liu F, Jiang F, *et al*. Synthesis and evaluation of 4-(2-hydroxypropyl) piperazin-1-yl) derivatives as Hsp90 inhibitors. Bioorg Med Chem. 2016;24(11):2423-2432. DOI: 10.1016/j.bmc.2016.03.049.
10. Hadden MK, Hill SA, Davenport J, Matts RL, Blagg BSJ. Synthesis and evaluation of Hsp90 inhibitors that contain the 1, 4-naphthoquinone scaffold. Bioorg Med Chem. 2009;17(2):634-640. DOI: 10.1016/j.bmc.2008.11.064.
11. Taldone T, Zatorska D, Patel PD, Zong H, Rodina A, Ahn JH, *et al*. Design, synthesis, and evaluation of small molecule Hsp90 probes. Bioorg Med Chem. 2011;19(8):2603-2614. DOI: 10.1016/j.bmc.2011.03.013.
12. Xiao Y, Liu Y. Recent advances in the discovery of novel HSP90 inhibitors: an update from 2014. Curr Drug Targets. 2020;21(3):302-317. DOI: 10.2174/1389450120666190829162544.
13. Sharp SY, Prodromou C, Boxall K, Powers M V, Holmes JL, Box G, *et al*. Inhibition of the heat shock protein 90 molecular chaperone *in vitro* and *in vivo* by novel, synthetic, potent resorcinylic pyrazole/isoxazole amide analogues. Mol Cancer Ther. 2007;6(4):1198-1211. DOI: 10.1158/1535-7163.MCT-07-0149.
14. Çalışkan B, Sinoplu E, İbiş K, Akhan Güzelcan E, Çetin Atalay R, Banoglu E. Synthesis and cellular bioactivities of novel isoxazole derivatives incorporating an arylpiperazine moiety as anticancer agents. J Enzyme Inhib Med Chem. 2018;33(1):1352-1361. DOI: 10.1080/14756366.2018.1504041.
15. Trivedi J, Parveen A, Rozy F, Mitra A, Bal C, Mitra D, Sharon A. Discovery of 2-isoxazol-3-yl-acetamide analogues as heat shock protein 90 (HSP90) inhibitors with significant anti-HIV activity. Eur J Med Chem. 2019;183:111699. DOI: 10.1016/j.ejmech.2019.111699.
16. Brough PA, Aherne W, Barril X, Borgognoni J, Boxall K, Cansfield JE, *et al*. 4, 5-diarylisoxazole Hsp90 chaperone inhibitors: potential therapeutic agents for the treatment of cancer. J Med Chem. 2008;51(2):196-218. DOI: 10.1021/jm701018h.
17. Abbasi M, Amanlou M, Aghaei M, Bakherad M, Doosti R, Sadeghi-Aliabadi H. New heat shock protein (Hsp90) inhibitors, designed by pharmacophore modeling and virtual screening: synthesis, biological evaluation and molecular dynamics studies. J Biomol Struct Dyn. 2020;38(12):3462-3473. DOI: 10.1080/07391102.2019.1660216.
18 Keshavarzipour F, Abbasi M, Khorsandi Z, Ardestani M, Sadeghi-Aliabadi H. Design, synthesis and biological studies of new isoxazole compounds as potent Hsp90 inhibitors. Scientific Reports. 2024;14(1):28017. DOI: 10.1038/s41598-024-79051-5.
19. Morris GM, Huey R, Lindstrom W, Sanner MF, Belew RK, Goodsell DS, *et al*. AutoDock4 and AutoDockTools4: automated docking with selective receptor flexibility. J Comput Chem. 2009;30(16):2785-2791. DOI: 1002/jcc.21256.
20. Bera AK, Kim KH. Full wwPDB X-ray Structure Validation Report. wwPDB. Available at: https://www.wwpdb.org/validation/2017/XrayValidationReportHelp
21. Azizian H, Bahrami H, Pasalar P, Amanlou M. Molecular modeling of *Helicobacter pylori* arginase and the inhibitor coordination interactions. J Mol Graph Model. 2010;28(7):626-235. DOI: 10.1016/j.jmgm.2009.12.007.
22. Makarewicz T, Kaźmierkiewicz R. Molecular dynamics simulation by GROMACS using GUI plugin for PyMOL. J Chem Inf Model. 2013;53(5):1229-1234. DOI: 10.1021/ci400071x.
23. Makarewicz T, Kaźmierkiewicz R. Improvements in GROMACS plugin for PyMOL, including implicit solvent simulations and displaying results of PCA analysis. J Mol Model. 2016;22(5):109,1-7. DOI: 10.1007/s00894-016-2982-4.
24. Pronk S, Páll S, Schulz R, Larsson P, Bjelkmar P, Apostolov R, *et al*. GROMACS 4.5: a high-throughput and highly parallel open source molecular simulation toolkit. Bioinformatics. 2013;29(7): 845-854. DOI: 10.1093/bioinformatics/btt055.
25. Søndergaard CR, Olsson MH, Rostkowski M, Jensen JH. Improved treatment of ligands and coupling effects in empirical calculation and rationalization of pKa values. J Chem Theory Comput. 2011;*7*(7): 2284-2295. DOI: 10.1021/ct200133y
26. Sousa da Silva, Alan W., and Wim F. Vranken. ACPYPE-Antechamber Python parser interface. BMC Res Notes. 2012;5:367,1-8. DOI: 10.1186/1756-0500-5-367.
27. Lagardère P, Mustière R, Amanzougaghene N, Hutter S, Franetich JF, Azas N, *et al*. 4-Substituted thieno [3, 2-d] pyrimidines as dual-stage antiplasmodial derivatives. Pharmaceuticals. 2022;15(7):820. DOI: 10.3390/ph15070820.
28. Ushijima S, Togo H. Metal-free one-pot conversion of electron-rich aromatics into aromatic nitriles. Synlett. 2010;2010(7):1067-1070. DOI: 10.1055/s-0029-1219575.
29. Johnson L, Powers J, Ma F, Jendza K, Wang B, Meredith E, *et al*. A reliable synthesis of 3-amino-5-alkyl and 5-amino-3-alkyl isoxazoles. Synthesis (Stuttg). 2013;45(2):171-173. DOI: 10.1055/s-0032-1317935.
30. Hassanzadeh F, Sadeghi-Aliabadi H, Jafari E, Sharifzadeh A, Dana N. Synthesis and cytotoxic evaluation of some quinazolinone- 5-(4-chlorophenyl) 1, 3, 4-oxadiazole conjugates. Res Pharm Sci. 2019;14(5):408-413. DOI: 10.4103/1735-5362.268201.

31. Hsanzadeh F, Jafari E, Shojaei F, Sadeghi-aliabadi H. Synthesis and cytotoxic activity evaluation of some new 1, 3, 4-oxadiazole, 1, 3, 4-thiadiazole and 1, 2, 4- triazole derivatives attached to phthalimide. Res Pharm Sci. 2021;16(6):634-642. DOI: 10.4103/1735-5362.327509.
32. Abbasi M, Amanlou M, Aghaei M, Hassanzadeh F, Sadeghi-Aliabadi H. Identification of new Hsp90 inhibitors: structure based virtual screening, molecular dynamic simulation, synthesis and biological evaluation. Anticancer Agents Med Chem. 2021;21(18):2583-2591. DOI: 10.2174/1871520621666210201101818.
33. Vilsmeier A, Haack A. Über die Einwirkung von Halogenphosphor auf Alkyl-formanilide. Eine neue Methode zur Darstellung sekundärer und tertiärer p-Alkylamino-benzaldehyde. Ber Dtsch Chem Ges. 1927;60(1):119-122. DOI: 10.1002/cber.19270600118.
34. Rodrigues FC, Kumar NVA, Hari G, Smith J, Lee K, Johnson M, *et al*. The inhibitory potency of isoxazole-curcumin analogue for the management of breast cancer: a comparative *in vitro* and molecular modeling investigation. Chem Pap. 2021;75(6):5995-6008. DOI: 10.1007/s11696-021-01775-9.
35. Balaji E, HariBabu B, Rao V, Subbaraju G, Nagasree K, Kumar M. Synthesis, screening and docking analysis of Hispolon pyrazoles and isoxazoles as potential antitubercular agents. Curr Top Med Chem. 2019;19(9):662-682. DOI: 10.2174/1568026619666190305124954.
36. Yin L, Niu C, Liao LX, Dou J, Habasi M, Aisa HA. An isoxazole chalcone derivative enhances melanogenesis in B16 melanoma cells via the Akt/GSK3β/β-catenin signaling pathways. Molecules. 2017;22(12):2077. DOI: 10.3390/molecules22122077.
37. Taha DE, Mahdi MF, Raauf AMR. Molecular modeling, synthesis, and antiproliferative evaluation of new isoxazole ring linked by Schiff bases and azo bond. J Adv Pharm Technol Res. 2023;14(3):213-219. DOI: 10.4103/japtr.japtr_170_23.
38. Mohamady S, Ismail MI, Mogheith SM, Attia YM, Taylor SD. Discovery of 5-aryl-3-thiophen-2-yl-1H-pyrazoles as a new class of Hsp90 inhibitors in hepatocellular carcinoma. Bioorganic Chem. 2020;94:103433. DOI: 10.1016/j.bioorg.2019.103433.
39. Ngu CP, Sahu R, Shah K, Paliwal D, Sah AK, Prajapati BG. Recent development in synthesis and anticonvulsant activity of promising Schiff base derivatives. J Heterocyclic Chem. 2025;62:1264-1284. DOI: 10.1002/jhet.70073.
40. Hamed MM, Abou El Ella DA, Keeton AB, Piazza GA, Abadi AH, Hartmann RW *et al*. 6-Aryl and heterocycle quinazoline derivatives as potent EGFR inhibitors with improved activity toward gefitinib-sensitive and -resistant tumor cell lines. J Med Chem. 2013;8(9):1495-1504. DOI: 10.1002/cmdc.201300147.
41. Lasri J, Eltayeb NE, Soliman SM, Ali EMM, Alhayyani S, Akhdhar A. Synthesis, crystal structure, DFT, and anticancer activity of some imine-type compounds via routine Schiff base reaction: an example of unexpected cyclization to oxazine derivative. Molecules. 2023;28(12):4766. DOI: 10.3390/molecules28124766.
42. Liu J, Wang F, Ma Z, Wang X, Wang Y. Structural determination of three different series of compounds as Hsp90 inhibitors using 3D-QSAR modeling, molecular docking and molecular dynamics methods. Int J Mol Sci. 2011;12(2):946-970. DOI: 10.3390/ijms12020946.
43. Bakherad Z, Mohammadi-Khanaposhtani M, Sadeghi-Aliabadi H, Rezaei S, Fasihi A, Bakherad M, *et al*. New thiosemicarbazide-1,2,3-triazole hybrids as potent α-glucosidase inhibitors: design, synthesis, and biological evaluation. J Mol Struct. 2019;1192:192-200. DOI: 10.1016/j.molstruc.2019.04.082.
44. Chandavaram PS, Maddirala SJ, Vidavalur S, Somaiah N. Design, synthesis and biological evaluation of isoxazole bearing N-arylpyrazole derivatives as anticancer agents. Chem Data Coll. 2022;41:100938. DOI: 10.1016/j.cdc.2022.100938.
45. Sharp SY, Prodromou C, Boxall K, Powers MV, Holmes JL, Box G, *et al*. Inhibition of the heat shock protein 90 molecular chaperone *in vitro* and *in vivo* by novel, synthetic, potent resorcinylic pyrazole/isoxazole amide analogues. Mol Cancer Ther. 2007;6(4):1198-1211. DOI: 10.1158/1535-7163.
46. Sun J, Lin C, Qin X, Dong X, Tu Z, Tang F, Chen C, Zhang J. Synthesis and biological evaluation of 3,5-disubstituted-4-alkynylisoxozales as a novel class of HSP90 inhibitors. Bioorg Med Chem Lett. 2015;25(16):3129-3134. DOI: 10.1016/j.bmcl.2015.06.009.
47. Wang X, Song X, Zhuo W, Fu Y, Shi H, Liang Y, *et al*. Advances in Hsp90 inhibitors for cancer therapy. Eur J Med Chem. 2021;218:113383. DOI: 10.1016/j.ejmech.2021.113383.
48. Sadeghi-Aliabadi H, Mirian M, Banizaman A, Rezazadeh M, Rahimi F, Sepahi S, Sadeghi-Aliabadi M. Gold nanoparticles from Artemisia absinthium, Morus nigra, and Peganum harmala: biosynthesis, characterization, and their biological evaluations against cancer cells. Res Pharm Sci. 2025;20(4): 485-497. DOI: 10.4103/RPS.RPS_159_23.